

Vortex Properties of a Resonant Superfluid

Meng Gao, Hongyu Wu, and Lan Yin*

School of Physics, Peking University, Beijing 100871, P. R. China

(Dated: May 8, 2006)

Abstract

The properties of a vortex in a rotating superfluid Fermi gas are studied in the unitary limit. A phenomenological approach based on Ginzburg-Landau theory is developed for this purpose. The density profiles, including those of the normal fluid and superfluid, are obtained at various temperatures and rotation frequencies. The superfluid and normal fluid densities can be identified from the angular momentum density. The total free energy and angular momentum of the vortex are also obtained.

*Electronic address: yinlan@pku.edu.cn

I. INTRODUCTION

The field of BEC-BCS crossover has attracted great attention from both experimental and theoretical sides. In experiments, the system is studied near Feshbach resonances so that the scattering length can be tuned by an applied magnetic field. At low temperatures, when the scattering length is tuned from negative side to positive side, the system evolves from a BCS state to a molecular BEC state. The observation of molecular BEC was first reported in references [1, 2]. When the scattering length was fast tuned from the negative side to the positive side of the resonance, condensation of Fermion pairs was observed [3, 4]. Since then quite a few experiments have focused on various properties of the system, including collective excitations [5, 6], single-particle excitations [7, 8], and thermodynamic properties [9]. The observation of vortex lattice [10] has provided a conclusive evidence of superfluidity across the resonance in this system.

The vortex structure in superfluid fermi gas have been studied theoretically [11, 12, 13, 14, 15, 16, 17, 18]. However most of these works focus on the non-rotating case, which is different from the experimental situation. To consider the effect of rotation, we have developed a phenomenological approach, based on our previous work on the phase-slip phenomenon in the resonant Fermi superfluid [19].

In this paper, we focus on the properties of a vortex in the unitary limit [20], because it is a special strong-interaction region where the magnitude of the scattering length is much bigger than the interparticle distance. In the unitary limit, the interparticle distance replaces the scattering length as the most important length scale, and the physical properties become unitary. In the following, we first present our phenomenological approach and then study the vortex structure at various temperatures and rotation frequencies.

II. FORMALISM

In our previous work [19], we developed a phenomenological theory for the resonant Fermi superfluid based on Ginzburg-Landau theory. To consider the effect of rotation, we study the system in the rotating frame, in which the single-particle Hamiltonian is given by

$$H - \Omega L_z = \frac{1}{2m}(p_\perp^2 + p_z^2) + \frac{1}{2}m(\omega_\perp^2 r_\perp^2 + \omega_z z^2) - \Omega \hat{\mathbf{z}} \cdot \mathbf{r}_\perp \times \mathbf{p}_\perp, \quad (1)$$

where $\mathbf{p}_\perp = (p_x, p_y, 0)$, $\mathbf{r}_\perp = (x, y, 0)$, ω_\perp and ω_z are the transverse and longitudinal trapping frequencies, and Ω is the rotation frequency. Here the trapping potential is assumed to have the rotation symmetry in the transverse plane. The single-particle Hamiltonian can be rewritten as

$$H - \Omega L_z = \frac{1}{2m}(\mathbf{p} - \frac{e\mathbf{A}}{c})^2 + \frac{1}{2}m[(\omega_\perp^2 - \Omega^2)r_\perp^2 + \omega_z^2z^2], \quad (2)$$

where $\mathbf{p} - e\mathbf{A}/c$ is the canonical momentum, and $e\mathbf{A}/c = m\Omega\hat{z} \times \mathbf{r}_\perp$. From Eq. (2), we conclude that the motion of a charge-neutral fermion in a rotating frame is analogous to an electron moving in a vector potential \mathbf{A} and in a trapping potential reduced in the transverse direction.

In the superfluid state, the free energy of a fermi gas is lower than that in the normal state, and the energy difference is defined as the condensation energy. The total free energy F is the sum of condensation energy F_C and the free energy of the normal state F_N ,

$$F = F_C + F_N. \quad (3)$$

The free energy of the normal state F_N is generally a complicated function of temperature, particle density, trapping potential, the scattering length, and the rotation frequency. According to Ginzburg-Landau theory, the condensation energy can be expressed as a functional of the vector potential \mathbf{A} and the order parameter ϕ which is proportional to the energy gap of the fermion excitation,

$$F_C = \int d^3r \left[-\frac{\hbar^2}{2m} \phi^*(\mathbf{r}) \left(\nabla - \frac{2ie\mathbf{A}}{\hbar c} \right)^2 \phi(\mathbf{r}) + \alpha(\mathbf{r}) |\phi(\mathbf{r})|^2 + \frac{\beta(\mathbf{r})}{2} |\phi(\mathbf{r})|^4 \right], \quad (4)$$

where α and β are coefficients. Although Ginzburg-Landau theory was originally proposed for describing superconducting system near the transition, it can often be applied to most of the region below the transition temperature.

When the system is not rotating, $\Omega = 0$, the sign change of the coefficient α signals the superfluid transition. Below the transition temperature T_C , $\alpha < 0$, and the system has lower free energy in the superfluid state than in the normal state. When the system is rotating, the transition temperature becomes a function of the rotation frequency Ω . In the following, the symbol T_C is defined as the transition temperature at $\Omega = 0$.

In the superfluid state, the total free energy F is at a minimum point as a functional of the particle density $n(\mathbf{r})$ and the superfluid order parameter $\phi(\mathbf{r})$,

$$\frac{\delta F}{\delta \phi^*(\mathbf{r})} = 0, \quad (5)$$

$$\frac{\delta F}{\delta n(\mathbf{r})} = 0. \quad (6)$$

In Eq. (6), the derivative is taken under the constraint of constant total-particle number. In principle, if the free energy F is known, the distributions of particle density and order parameter in the superfluid state can be solved from the saddle point equations, Eq. (5, 6).

At low temperatures and low rotation frequencies, when the Fermi energy is much bigger than rotation energy, $E_F \gg \hbar\Omega$, the average kinetic energy per particle is proportional to $n^{2/3}(\mathbf{r})$ in the Thomas-Fermi approximation [21]. In the unitary limit, the interparticle distance replaces the scattering length, and the average interaction energy is also proportional to $n^{2/3}(\mathbf{r})$. Therefore the free energy of the normal state is approximately given by

$$F_N \approx \int d^3r \left[\frac{\hbar^2}{2m} c_N n^{\frac{5}{3}}(\mathbf{r}) + V'(\mathbf{r}) n(\mathbf{r}) \right], \quad (7)$$

where $V'(\mathbf{r}) \equiv m[(\omega_{\perp}^2 - \Omega^2)r_{\perp}^2 + \omega_z z^2]/2$ is the trapping potential reduced due to rotation, and c_N is a dimensionless constant. From the experiment [22], the constant c_N is estimated to be about 4.3. At low rotation frequencies, $E_F \gg \hbar\Omega$, the constant c_N does not depend on the rotation frequency Ω . In general, the normal-state free energy F_N should be temperature dependent. However, near the transition temperature which is much smaller than the Fermi temperature [7], the normal-state free energy F_N is weakly dependent on the temperature and the coefficient c_N is approximately temperature independent.

In the unitary limit, the coefficients α and β in Eq. (4) can be expressed in terms of the particle density n and temperature T . The coefficient α is approximately given by $\alpha = c_{\alpha} k_B (T - T_C)$, where c_{α} is a dimensionless constant and k_B is the Boltzmann constant. The coefficient β is a function of the fermion density, $\beta = c_{\beta} \hbar^2 / [2mn^{1/3}]$, where c_{β} is a dimensionless constant. The transition temperature in the unitary limit is proportional to $n^{2/3}$, $k_B T_C = c_T \hbar^2 n^{2/3} / (2m)$, where c_T is a dimensionless constant. In the experiment [7], the transition temperature T_C is about 25% of the Fermi temperature T_F , corresponding to $c_T = 2.4$. Although the zero-temperature properties of the unitary Fermi gas has been numerically obtained [23], the accurate values of the constants c_{α} and c_{β} near the transition temperature are still unknown. In the following, we use their values in the weak-interaction case instead, $c_{\alpha} = 1.47 c_T$ and $c_{\beta} = 2.94 c_T^2$ [24], and discuss how these parameters affect the system properties near the end. In the unitary limit, the saddle-point equations (5, 6) can

be further written as

$$-\frac{\hbar^2}{2m}(\nabla - \frac{2ie\mathbf{A}}{\hbar c})^2\phi(\mathbf{r}) + \alpha(\mathbf{r})\phi(\mathbf{r}) + \beta(\mathbf{r})|\phi(\mathbf{r})|^2\phi(\mathbf{r}) = 0, \quad (8)$$

$$\frac{5\hbar^2}{6m}c_Nn^{2/3}(\mathbf{r}) + V'(\mathbf{r}) - \mu - \frac{\hbar^2}{3m}c_Tc_\alpha\frac{|\phi(\mathbf{r})|^2}{n^{1/3}(\mathbf{r})} - \frac{\hbar^2}{12m}c_\beta\frac{|\phi(\mathbf{r})|^4}{n^{4/3}(\mathbf{r})} = 0, \quad (9)$$

where μ is the chemical potential.

The angular momentum can be obtained from the free energy, $L_z = -\partial F/\partial\Omega$. In the unitary limit, it is given by

$$L_z = \int d^3r[m\Omega r_\perp^2 n(\mathbf{r}) + 2\phi^*(\mathbf{r})(\hat{z} \times \mathbf{r}_\perp) \cdot (-i\hbar\nabla - \frac{2e\mathbf{A}}{c})\phi(\mathbf{r})] \quad (10)$$

$$= \int d^3r\{m\Omega r_\perp^2[n(\mathbf{r}) - 4|\phi(\mathbf{r})|^2] - 2i\hbar\phi^*(\mathbf{r})\frac{\partial}{\partial\theta}\phi(\mathbf{r})\}, \quad (11)$$

where θ is the azimuthal angle around \hat{z} -axis. When there is no superfluid current, the phase of the order parameter is uniform and the angular momentum totally comes from the normal fluid,

$$L_z = \int d^3r m\Omega r_\perp^2[n(\mathbf{r}) - 4|\phi(\mathbf{r})|^2]. \quad (12)$$

Therefore we identify $n_n(\mathbf{r}) \equiv n(\mathbf{r}) - 4|\phi(\mathbf{r})|^2$ as the density of the normal fluid and $n_s(\mathbf{r}) \equiv 4|\phi(\mathbf{r})|^2$ as the superfluid density. In rotating systems, if the density of the angular momentum can be measured experimentally, the superfluid and normal fluid densities can be obtained from Eq. (11).

III. VORTEX STRUCTURE AND THERMODYNAMICAL PROPERTIES

In a single-vortex state, the order parameter takes the form $\phi(\mathbf{r}) = f(r_\perp, z)e^{i\theta}$, where for convenience f can be chosen as a positive function, $f = |\phi|$. The order parameter and particle density of the vortex state can be obtained from the saddle-point equations (8, 9) which can now be further simplified,

$$-\frac{\hbar^2}{2m}\left(\frac{1}{r_\perp}\frac{\partial f}{\partial r_\perp} + \frac{\partial^2 f}{\partial r_\perp^2} + \frac{\partial^2 f}{\partial z^2} - \frac{f}{r_\perp^2}\right) + 2m\Omega^2 r_\perp^2 f - 2\hbar\Omega f + \alpha f + \beta f^3 = 0, \quad (13)$$

$$\frac{5\hbar^2}{6m}c_Nn^{2/3} + V' - \mu - \frac{\hbar^2}{3m}c_Tc_\alpha\frac{f^2}{n^{1/3}} - \frac{\hbar^2}{12m}c_\beta\frac{f^4}{n^{4/3}} = 0. \quad (14)$$

The angular momentum in the vortex state can be obtained from Eq. (11),

$$L_z = \int d^3r[m\Omega r_\perp^2(n - 4f^2) + 2\hbar f^2]. \quad (15)$$

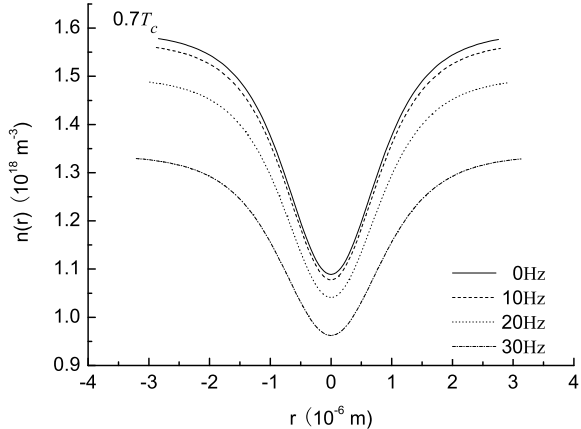


FIG. 1: The density profile of the vortex at $T = 0.7T_C$ and $z = 0$. The solid, dashed, dotted, and dotted dash lines are density profiles at rotating frequency 0Hz, 10Hz, 20Hz, and 30Hz.

From Eq. (15), we can see that in a single-vortex state each superfluid particle contributes $\hbar/2$ to the total angular momentum.

To solve the nonlinear differential equations Eq. (13) and (14), it is necessary to use the numerical method. Here we take the experimental parameters from Ref. [10], in which the average number of Li^6 atoms is about two million, $N \approx 2 \times 10^6$, the axial and radial trap frequencies are given by $\nu_z = 23\text{Hz}$ and $\nu_r = 57\text{Hz}$. The nonlinear partial differential equations (13) and (14) are solved by the iteration method.

In Fig. (1), the density profiles of the vortex are plotted at $T = 0.7T_C$ and different rotation frequencies. The vortex produces a density dip at the center and the normal fluid is dominant inside the vortex core. This is because the superfluid density vanishes at the center, as shown in Fig. (2). At very low rotation frequencies, from Eq. (13) the size of the vortex core is given by $\xi = \hbar/\sqrt{-2m\alpha(0)}$. When the rotation frequency increases, the density decreases near the center of the trap as shown in Fig. (1), due to the increase of the centrifugal force. When the density decreases, the coefficients α and β in the Ginzburg-Landau theory increase, and from Eq. (13) the size of the order parameter decreases. As a result, the superfluid density also decreases with the increase of the rotation frequency, and the size of the vortex core increases, as shown in Fig. (2).

When the temperature increases, the superfluid density decreases as shown in Fig. (3). The size of the vortex core becomes larger because the coefficient α increases with the

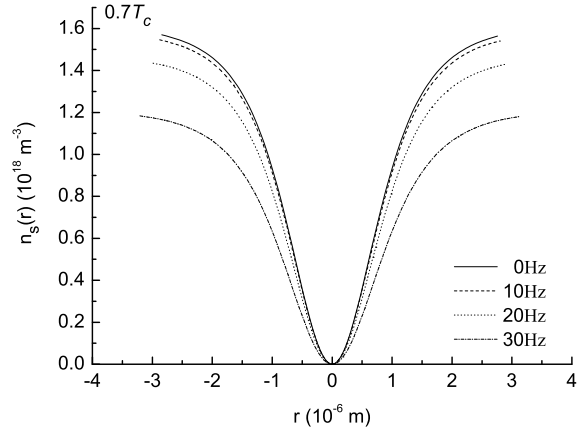


FIG. 2: The superfluid density profile at $T = 0.7T_C$ and $z = 0$. The solid, dashed, dotted, and dotted dash lines are superfluid density profiles at rotating frequency 0Hz, 10Hz, 20Hz, and 30Hz.

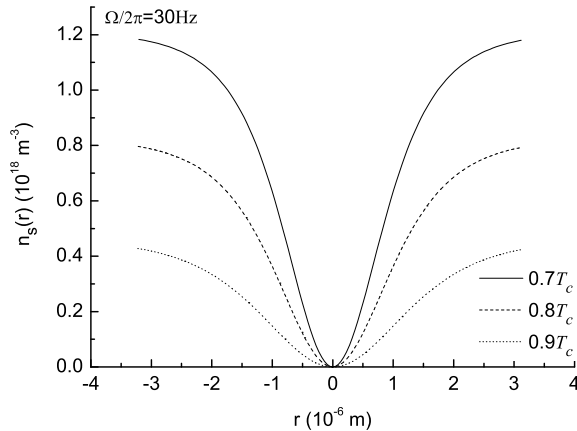


FIG. 3: The superfluid density profile at $\Omega/(2\pi) = 30\text{Hz}$ and $z = 0$. The solid, dashed, and dotted lines are superfluid density profiles at $0.7T_C$, $0.8T_C$, and $0.9T_C$.

increase of temperature. The density close to the vortex core also decreases as shown in Fig. (4). To keep the total particle number constant, the densities at other places increase. As a result, the density at the center slightly increases with the increase of temperature.

The total free energy as a function of the rotation frequency is plotted in Fig. (5). As the rotation frequency increases, the free energy decreases mainly due to the reduction of the trapping potential. As the temperature increases, the free energy also increases. In contrast, the absolute value of the condensation energy decreases with the increase of temperature as

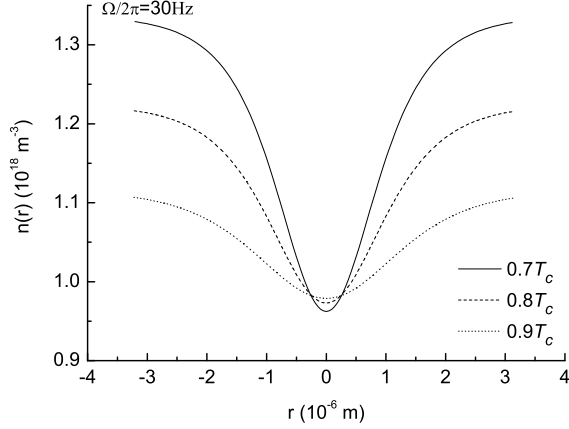


FIG. 4: The density profile of the vortex at $\Omega/(2\pi) = 30\text{Hz}$ and $z = 0$. The solid, dashed, and dotted lines are the density profiles at $0.7T_C$, $0.8T_C$, and $0.9T_C$.

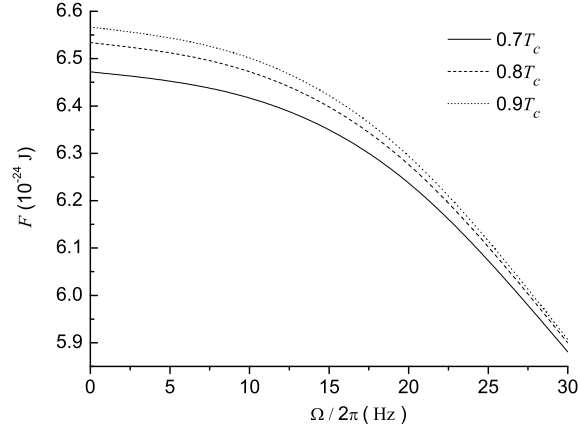


FIG. 5: The total free energy as a function of rotation frequency. The solid, dashed, and dotted lines are free energies at $0.7T_C$, $0.8T_C$, and $0.9T_C$.

shown in Fig. (6). The absolute value of the condensation energy also decreases with the increase of rotation frequency due to the decrease of the total superfluid fraction as shown in Fig. (7). The total angular momentum almost increases linearly with the rotation frequency as shown in Fig. (8). The linear dependence comes from the normal fluid contribution, and in contrast the superfluid in the vortex state contributes a small constant to the total angular momentum.

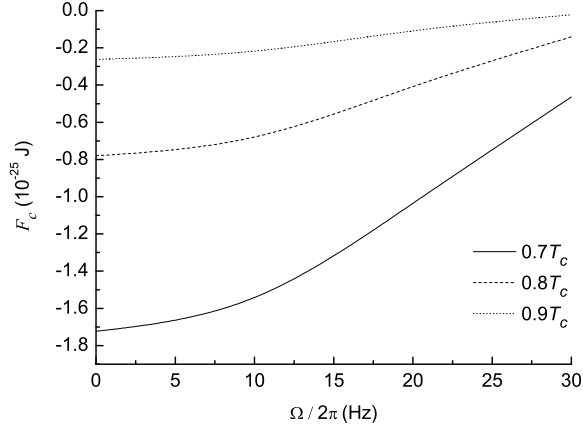


FIG. 6: The condensation energy as a function of rotation frequency. The solid, dashed, and dotted lines are condensation energies at $0.7T_c$, $0.8T_c$, and $0.9T_c$.

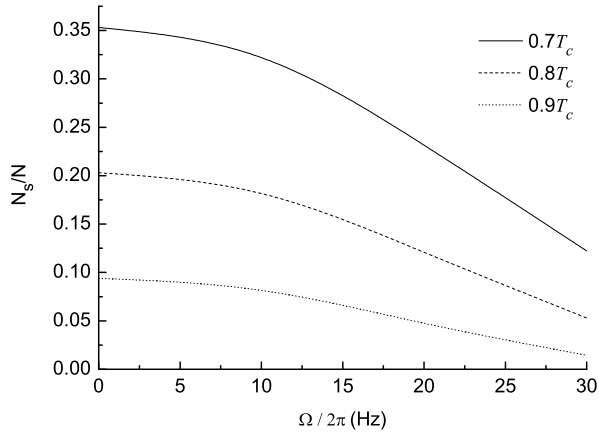


FIG. 7: The superfluid fraction as a function of rotation frequency. The solid, dashed, and dotted lines are the ratios of the superfluid atom number to total atom number at $0.7T_c$, $0.8T_c$, and $0.9T_c$.

IV. DISCUSSION AND CONCLUSION

So far we use the weak-interaction expressions of the parameters c_α and c_β to obtain vortex properties. It is likely that the accurate expressions of these parameters in the unitary limit are different. Here we examine how sensitive the vortex properties are to these parameters. In Fig. (9), the density profiles of the vortex at $T = 0.9T_c$ with various values of c_α and c_β

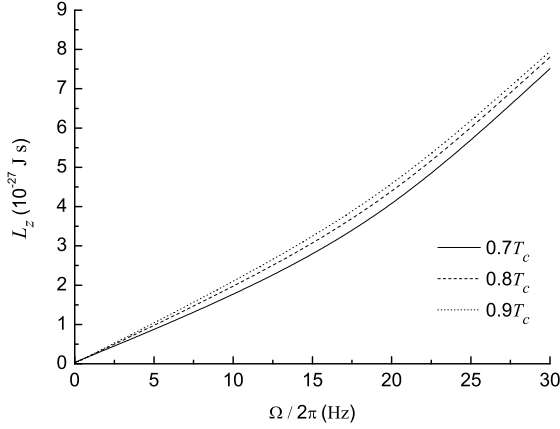


FIG. 8: The total angular momentum as a function of rotation frequency. The solid, dashed, and dotted lines are the angular momentum at $0.7T_C$, $0.8T_C$, and $0.9T_C$.

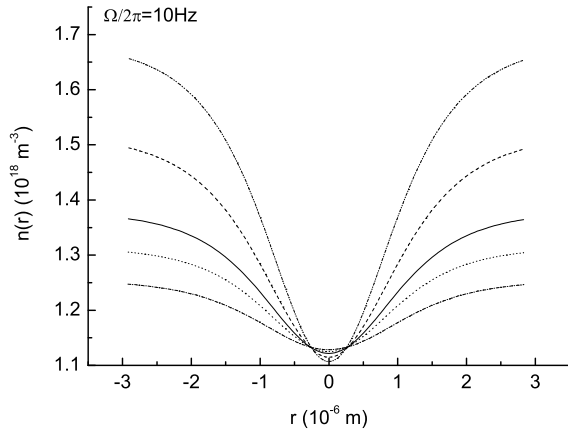


FIG. 9: The density profile at $T = 0.9T_C$ and $\Omega/(2\pi) = 10\text{Hz}$. The solid line is the density profile with the weak-interaction expressions of c_α and c_β . The dotted-dash and double-dotted-dashed lines are the density profiles with c_α decreased and increased by 20% respectively. The dashed and dotted lines are the density profiles with c_β decreased and increased by 20% respectively.

are plotted. As shown in Fig. (9), when c_α increases or c_β decreases, the dip at the center of the vortex becomes bigger. This is due to the increase of order parameter and the increase of the absolute value of the condensation energy as shown in Fig. (10). If the vortex structure can be measured in the experiment, the values of the parameters c_α and c_β can be pinned down, which is very helpful to obtain other properties of the system.

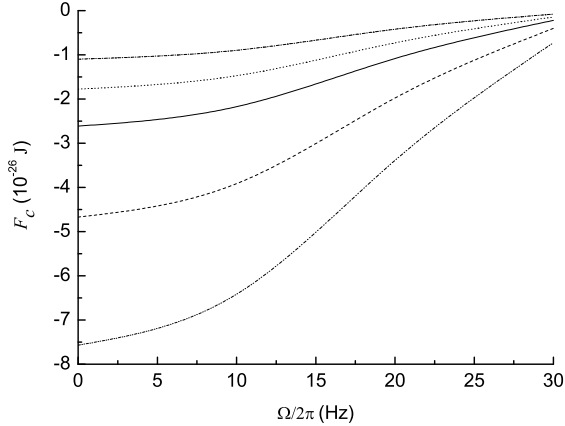


FIG. 10: The condensation energy at $T = 0.9T_C$ as a function of Ω . The solid line is the condensation energy with the weak-interaction expressions of c_α and c_β . The dotted-dash and double-dotted-dashed lines are the condensation energies with c_α decreased and increased by 20% respectively. The dashed and dotted lines are the condensation energies with c_β decreased and increased by 20% respectively.

In summary, we have developed a phenomenological theory to study the vortex properties of a superfluid Fermi gas in the unitary region. This charge-neutral system under rotation is mapped onto an electron system in a vector potential. In the framework of the Ginzburg-Landau theory, the order-parameter and density distributions in the equilibrium state are solved numerically from the saddle-point equations of the free energy. We identify that the superfluid density is four times the magnitude of the order parameter squared, which can be determined from the angular-momentum density. The size of the vortex core is found to increase with the rotation frequency due to the density decrease near the core. Thermodynamical properties of the vortex, such as the free energy and angular momentum, are also obtained. Our theoretical results can be directly tested in experiments.

Although the vortex properties in the unitary region are studied extensively in this paper, more work are needed to study the rotation effect in other regions of the BEC-BCS crossover, such as the crossover region and the BEC side. It is also interesting to extend this phenomenological approach to study the properties of vortex lattices in the BEC-BCS crossover.

We would like to thank T.-L. Ho, P. Ao, and D.P. Li for helpful discussions. This work

is supported by NSFC under Grant No. 90303008.

- [1] S. Jochim *et al.*, *Science* **302**, 2101 (2003).
- [2] M. Greiner, C. A. Regal, and D. S. Jin, *Nature* **426**, 537 (2003).
- [3] C. A. Regal, M. Greiner, and D. S. Jin, *Phys. Rev. Lett.* **92**, 040403(2004).
- [4] M. W. Zwierlein *et al.*, *Phys. Rev. Lett.* **92**, 120403 (2004).
- [5] J. Kinast, S. L. Hemmer, M. E. Gehm, A. Turlapov, and J. E. Thomas, *Phys. Rev. Lett.* **92**, 150402 (2004).
- [6] M. Bartenstein, A. Altmeyer, S. Riedl, S. Jochim, C. Chin, J. H. Denschlag, and R. Grimm, *Phys. Rev. Lett.* **92**, 203201(2004).
- [7] C. Chin, M. Bartenstein, A. Altmeyer, S. Riedl, S. Jochim, J. Hecker-Denschlag, and R. Grimm, *Science* **305**, 1128(2004).
- [8] M. Greiner, C. A. Regal, and D. S. Jin, *PRL* **94**, 070403(2005).
- [9] J. Kinast, A. Turlapov, J. E. Thomas, Q. J. Chen, J. Stajic, and K. Levin, *Science* **307**, 1296 (2005).
- [10] M. W. Zwierlein, et. al, *Nature* **435**, 1047 (2005).
- [11] G. M. Bruun and L. Viverit, *Phys. Rev. A* **64**, 063606(2001).
- [12] M. Rodriguez, and G. -S. Paraoanu, and P. Törmä, *Phys. Rev. Lett.* **87**, 100402(2001).
- [13] N. Nygarrd, G. M. Bruun, C. W. Clark, and D. L. Feder, *Phys. Rev. Lett.* **90**, 210402(2003).
- [14] A. Bulgac and Y. Yu, *Phys. Rev. Lett.* **91**, 190404(2003).
- [15] N. Nygarrd, G. M. Bruun, B. I. Schneider, C. W. Clark and D. L. Feder, *Phys. Rev. A* **69**, 053622(2004).
- [16] J. Tempere, M. Wouters, and J. T. Devreese, *Phys. Rev. A* **71**, 033631(2005).
- [17] C. C. Chien, Y. He, Q. Chen, and K. Levin *Phys. Rev. A* **73**, 041603(R) (2006).
- [18] Rajdeep Sensarma, Mohit Randeria, and Tin-Lun Ho, *Phys. Rev. Lett.* **96**, 090403 (2006).
- [19] Lan Yin and Ping Ao, *Phys. Rev. A* **71**, 041603(R) (2005); Hongyu Wu and Lan Yin, *Acta Physica Sinica* **55**, 490 (2006).
- [20] T.-L. Ho, *Phys. Rev. Lett.* **92**, 090402 (2004).
- [21] T.-L. Ho and C. V. Ciobanu, *Phys. Rev. Lett.* **85**, 4648 (2000).
- [22] M. E. Gehm, S. L. Hemmer, S. R. Granade, K. M. O'Hara, and J. E. Thomas, *Phys. Rev. A*

68, 011401(R) (2003).

[23] J. Carlson, S.-Y. Chang, V. R. Pandharipande, and K. E. Schmidt, Phys. Rev. Lett. **91**, 050401 (2005).

[24] J. R. Schrieffer, *Theory of superconductivity* (Benjamin, Reading, 1964), chapter 8; V. N. Popov, *Functional integrals and collective excitations* (Cambridge University, Cambridge, 1987), chapter 13.